



**RESEARCH ARTICLE**

**INFLUENCE OF ZnO INCORPORATION ON PHASE STABILITY, MORPHOLOGY AND APPARENT DENSITY OF TiO<sub>2</sub>-BASED SPRAY FEEDSTOCK POWDERS**

**Muhamad Akmal Mohd Sani<sup>1</sup>, Yusliza Yusuf<sup>1,\*</sup>, Jariah Mohamad Juoi<sup>1</sup>, Azhar Shah Abu Hassan<sup>1</sup>, Sarita Morakul<sup>2</sup>**

<sup>1</sup>*Fakulti Teknologi Dan Kejuruteraan Industri Dan Pembuatan, Universiti Teknikal Malaysia Melaka, Hang Tuah Jaya, 76100 Durian Tunggal, Melaka, Malaysia.*

<sup>2</sup>*Department of Mechanical Engineering, Chulalongkorn University, Phayathai Road Pathumwan, Bangkok 10330, Thailand.*

**Abstract.** TiO<sub>2</sub> based ceramic coatings are extensively used in plasma spray applications due to their excellent hardness, wear resistance, and chemical stability. Nevertheless, the performance of plasma sprayed coatings is strongly influenced by the physical and microstructural characteristics of the feedstock powders. This study investigates the influence of ZnO incorporation on the phase composition, morphology, microstructure, particle distribution, and apparent density of TiO<sub>2</sub>-based plasma spray feedstock powders. ZnO was selected due to its favourable chemical compatibility and complementary physical properties with TiO<sub>2</sub>, which may enhance phase stability, particle cohesion, and powder packing behaviour. TiO<sub>2</sub> and ZnO powders were blended at different weight ratios of 90 wt.% TiO<sub>2</sub>/10 wt.% ZnO, 80 wt.% TiO<sub>2</sub>/20 wt.% ZnO, and 70 wt.% TiO<sub>2</sub>/30 wt.% ZnO using wet mixing followed by planetary ball milling without milling balls to promote homogeneous agglomeration while preserving particle integrity. X-ray diffraction (XRD) analysis confirmed the coexistence of anatase and rutile TiO<sub>2</sub> phases together with the ZnO wurtzite phase without the formation of secondary phases, indicating good phase compatibility and homogeneous ZnO distribution within the powder matrix. FESEM observations revealed angular and well-defined TiO<sub>2</sub> particles, while ZnO appeared as finer irregular aggregates distributed around the TiO<sub>2</sub> surfaces. Incorporation of 10 wt.% ZnO resulted in more uniform particle dispersion, reduced agglomeration, and improved packing through effective filling of interparticle voids. Apparent density analysis showed that moderate ZnO incorporation enhanced bulk density and packing efficiency, whereas excessive ZnO addition increased interparticle voids and reduced powder density. Among all compositions, the 90 wt.% TiO<sub>2</sub>/10 wt.% ZnO feedstock exhibited the most balanced combination of phase stability, morphology, and packing characteristics, demonstrating strong potential for dense and wear-resistant plasma-sprayed coating applications.

**Keywords:** ZnO, TiO<sub>2</sub>, plasma spraying, feedstock powder.

**Article Info**

Received 9 January 2026

Accepted 24 April 2026

Published 8 June 2026

**\*Corresponding author:** [yusliza@utem.edu.my](mailto:yusliza@utem.edu.my)

Copyright Malaysian Journal of Microscopy (2026). All rights reserved.

ISSN: 1823-7010, eISSN: 2600-7444

## 1. INTRODUCTION

Researchers have extensively investigated titanium dioxide (TiO<sub>2</sub>) as a valuable ceramic material because to its exceptional hardness, chemical inertness, corrosion resistance, and photocatalytic properties. Due to these advantageous properties, it is extensively utilised in industry for applications such as aircraft components, biomedical coatings, photocatalytic surfaces, and energy conversion devices. TiO<sub>2</sub> is a favoured option for coating technologies and surface protection systems due to its distinctive combination of mechanical and chemical stability [1-2].

Despite its advantages, pure TiO<sub>2</sub> coatings frequently exhibit issues such as brittleness, inadequate adhesion, and lack of durability upon fracture, particularly when applied to metal substrates. The primary causes of these issues are the significant disparity in thermal expansion between TiO<sub>2</sub> and metal surfaces [3], coupled with the inherent rigidity of TiO<sub>2</sub>. Consequently, these constraints diminish its utility in environments where durability and adhesion are critical, particularly in conditions characterised by abrasion and elevated temperatures. To address these challenges, researchers have investigated the incorporation of secondary oxide elements into TiO<sub>2</sub> to enhance its structural and functional efficacy [4]. The incorporation of appropriate oxides and other material can alter grain morphology, enhance microstructure, and increase the toughness and adhesion of the material. For instance, Al-TiO<sub>2</sub> and Al<sub>2</sub>O<sub>3</sub>-TiO<sub>2</sub> composite coatings have been reported to enhance coating density, adhesion strength, and wear resistance. However, these improvements are often system-specific and may introduce new challenges such as phase instability or processing complexity[5].

Zinc oxide (ZnO) has emerged as a compelling addition for TiO<sub>2</sub>-based systems due to its chemical compatibility and favourable physical properties that complement TiO<sub>2</sub> [2,6]. ZnO possesses a hexagonal wurtzite crystal structure that exhibits significant thermal and mechanical stability. Synthesis of TiO<sub>2</sub>-ZnO from its precursor also results in formation of ZnO Hexagonal Wurtzite phase (JCPDS Card No. 80-0075) [7]. The lattice characteristics and melting point are quite analogous to those of TiO<sub>2</sub>, facilitating the formation of solid solutions or composite phases during high-temperature processes. When combined with TiO<sub>2</sub>, ZnO enhances phase stability, improves particle cohesion, and facilitates a more uniform distribution of components within the powder matrix. The TiO<sub>2</sub>-ZnO composite system possesses the ability to enhance its functional properties with its mechanical benefits. Multiple investigations have shown enhancements in optical, electrical, and photocatalytic properties resulting from the incorporation of ZnO. Moreover, TiO<sub>2</sub>/ZnO complexes exhibit potential for use in wear-resistant and high-temperature coatings, using the lubricating properties of ZnO and the mechanical strength of TiO<sub>2</sub> [8].

This particular feedstock powder is meant to be used for plasma spray coating. There are existing paper that report on the use of TiO<sub>2</sub>/ZnO as coating material commonly due to its self cleaning, antibacterial properties and its high hardness properties [9]. However, many of the researchers uses different type of deposition method such as sol-gel process, physical vapor deposition and chemical vapor deposition. The coating material used is also vary, there are researchers that synthesize their own TiO<sub>2</sub> and ZnO while few use over the shelf ready made powder form [10]. There are few research papers that use plasma spray deposition method to deposit TiO<sub>2</sub>/ZnO coating onto substrate [11].

In plasma spraying, the properties of the feedstock powder play a decisive role in determining coating performance, including porosity, adhesion, and mechanical strength. Parameters such as particle size distribution, morphology, and apparent density directly affect powder flowability, melting behaviour, and deposition efficiency. An optimal particle size range (typically 15–45 µm) is essential to ensure uniform melting and consistent coating formation [12]. However, the relationship between ZnO content and these critical powder characteristics remains insufficiently understood, particularly in terms of packing efficiency and its impact on coating integrity.

This study investigates the effects of ZnO addition on the microstructure and phase composition of TiO<sub>2</sub>-based plasma spray feedstock powders. This study aims to clarify the relationship between composition and powder properties by systematically varying the TiO<sub>2</sub>/ZnO ratios and examining the

resulting powders by X-ray Diffraction (XRD), scanning electron microscopy (SEM), and particle size analysis (PSA). The results are expected to provide substantial insights for optimising TiO<sub>2</sub>/ZnO feedstock formulations, hence improving their suitability for plasma spray applications in advanced surface engineering.

## 2. MATERIALS AND METHODS

### 2.1 TiO<sub>2</sub> and ZnO powder

Oerlikon Metco (Switzerland) supplied titanium dioxide (TiO<sub>2</sub>) powder, marketed as Oerlikon Metco 102. This was the primary material utilized in this study. The powder consists of approximately 99 % titanium dioxide, with the remaining 1 % comprising trace amounts of other minerals such as alumina (Al<sub>2</sub>O<sub>3</sub>), iron oxide (Fe<sub>2</sub>O<sub>3</sub>), and silicon oxide (SiO<sub>2</sub>). The maker states that the powder appears dark grey due to its sub-stoichiometric composition (TiO<sub>x</sub>, where  $x < 2$ ). This non-stoichiometric characteristic indicates a slight deficiency of oxygen, which is known to alter the electrical and thermal properties of TiO<sub>2</sub>. The powder particles exhibit angular to irregular morphology, and their dimensions are suitable for thermal spray applications. Figure 1 illustrates the appearance of the TiO<sub>2</sub> powder upon initial receipt.



**Figure 1** : Metco 102 powder by Oerlikon as received

In this investigation, zinc oxide (ZnO) powder obtained from Tokyo Chemical Industry (TCI, Japan) as the secondary additive was employed. The molecular weight of the supplied ZnO is 81.38 g/mol, and the purity is 99 %, according to the manufacturer's specification document. The ZnO powder is composed of small, nearly spherical particles with an exceptionally uniform surface, as demonstrated in Figure 2. For the purpose of generating blended feedstock compositions for plasma spraying, both TiO<sub>2</sub> and ZnO powders were mixed. The final feedstock material's physical and structural characteristics were examined in relation to the ZnO content by combining the TiO<sub>2</sub>/ZnO granules in varying weight ratios.



**Figure 2:** ZnO powder as received

### ***2.2 Feedstock Powder Preparation***

The preparation of the TiO<sub>2</sub>/ZnO feedstock powder began by blending titanium dioxide (Metco 102, Oerlikon Metco) and zinc oxide (Tokyo Chemical Industry, Japan) at weight ratios of 90:10, 80:20, and 70:30, respectively. To enhance particle cohesion during mixing, a 5 wt.% polyvinyl alcohol (PVA) solution was employed as a temporary binder. For each 100 g batch of mixed powder, 50 ml of deionized water was added to ensure uniform wet mixing and binder distribution.

The blending process was carried out using a planetary ball mill (Retsch PM 100, Germany) operated at 200 rpm for 2 hours. No grinding media were used during the process, as the objective was solely to achieve homogeneous mixing without reducing particle size. Following mixing, the slurry-like mixture was oven-dried at 80 °C for 24 hours to remove residual moisture and promote powder agglomeration. The dried agglomerates were subsequently sieved through an 80-mesh stainless steel sieve to obtain uniform particle size distribution. The resulting TiO<sub>2</sub>/ZnO feedstock powders, ready for plasma spraying, are shown in Figure 3.



**Figure 3:** TiO<sub>2</sub>/ZnO feedstock powder for plasma spray process

### 2.3 Field Emission Scanning Electron Microscope (FESEM) analysis

Field emission scanning electron microscope (Model: Hitachi SU5000, Japan) was employed to examine the morphological characteristics of the TiO<sub>2</sub>/ZnO feedstock powders. The analysis focused on evaluating particle size, morphology, surface texture, and porosity, as these elements are critical in affecting powder flowability, packing properties, and melting efficiency in plasma spraying.

### 2.4 Phase and Structural Characterization

The crystalline structure and phase composition of the TiO<sub>2</sub>/ZnO feedstock powders were examined using x-ray diffraction (XRD) to identify the constituent phases and evaluate the effect of ZnO addition on structural evolution. The analysis was performed using a Rigaku MiniFlex diffractometer equipped with Cu K $\alpha$  radiation ( $\lambda = 1.5406 \text{ \AA}$ ), operated under a scanning range of  $2\theta = 20^\circ\text{--}80^\circ$ , with a step size of  $0.02^\circ$  and a scanning rate of  $1^\circ/\text{min}$ . Data acquisition and processing were conducted using SmartLab Studio II software, which provided high-resolution diffraction profiles for phase identification and comparison.

The obtained diffraction patterns were presented as intensity versus  $2\theta$  plots and were compared against reference data from the International Centre for Diffraction Data (ICDD) database to confirm the presence of TiO<sub>2</sub> (anatase and rutile) and ZnO (wurtzite) phases. Variations in peak position and intensity were carefully analyzed to detect possible compositional interactions, such as partial solid solution formation or lattice distortion, resulting from ZnO incorporation into the TiO<sub>2</sub> matrix. This structural assessment provided critical insights into the stability, crystallinity, and phase evolution of the mixed oxide powders intended for plasma spray feedstock applications.

### 2.5 Particle Size Distribution Analysis

In addition to phase and morphological analysis, the particle size distribution (PSD) of the powders was measured using a laser diffraction particle size analyzer (Model: Mastersizer 2000, Malvern Panalytical, UK). Laser diffraction was employed as it provides a reliable and reproducible method for characterizing particle size based on light scattering behavior. In this technique, a laser beam is directed through the powder suspension, and the angular distribution of the scattered light is analyzed where larger particles scatter light at smaller angles, while smaller particles scatter light at wider angles. The resulting PSD curves are expressed in terms of  $d(0.1)$ ,  $d(0.5)$ , and  $d(0.9)$  values, representing the particle diameter below which 10 %, 50 %, and 90 % of the sample volume lies, respectively. This analysis provides essential information on powder uniformity and flow characteristics, which directly influence the feedstock's performance during plasma spraying.

### 2.6 Apparent Density

The apparent (bulk) density of the TiO<sub>2</sub>/ZnO feedstock powders were measured to evaluate their suitability for plasma spray applications. Apparent density represents the mass of powder per unit bulk volume, including the void spaces between loosely packed particles. Measurements were performed following the ASTM B212 standard. Approximately 50 g of each powder sample was poured gently into a 50 mL graduated cylinder without compressing the material. The bulk volume of the powder was recorded, and the apparent density was calculated using the Equation 1.

$$\rho = \frac{m}{V} \quad (1)$$

where  $m$  is the mass of the powder (g) and  $V$  is the bulk volume (cm<sup>3</sup>). Each measurement was repeated three times to ensure reproducibility, and the mean and standard deviation were reported.

### 3. RESULTS AND DISCUSSION

#### 3.1 FESEM Micrograph of Powder Morphology

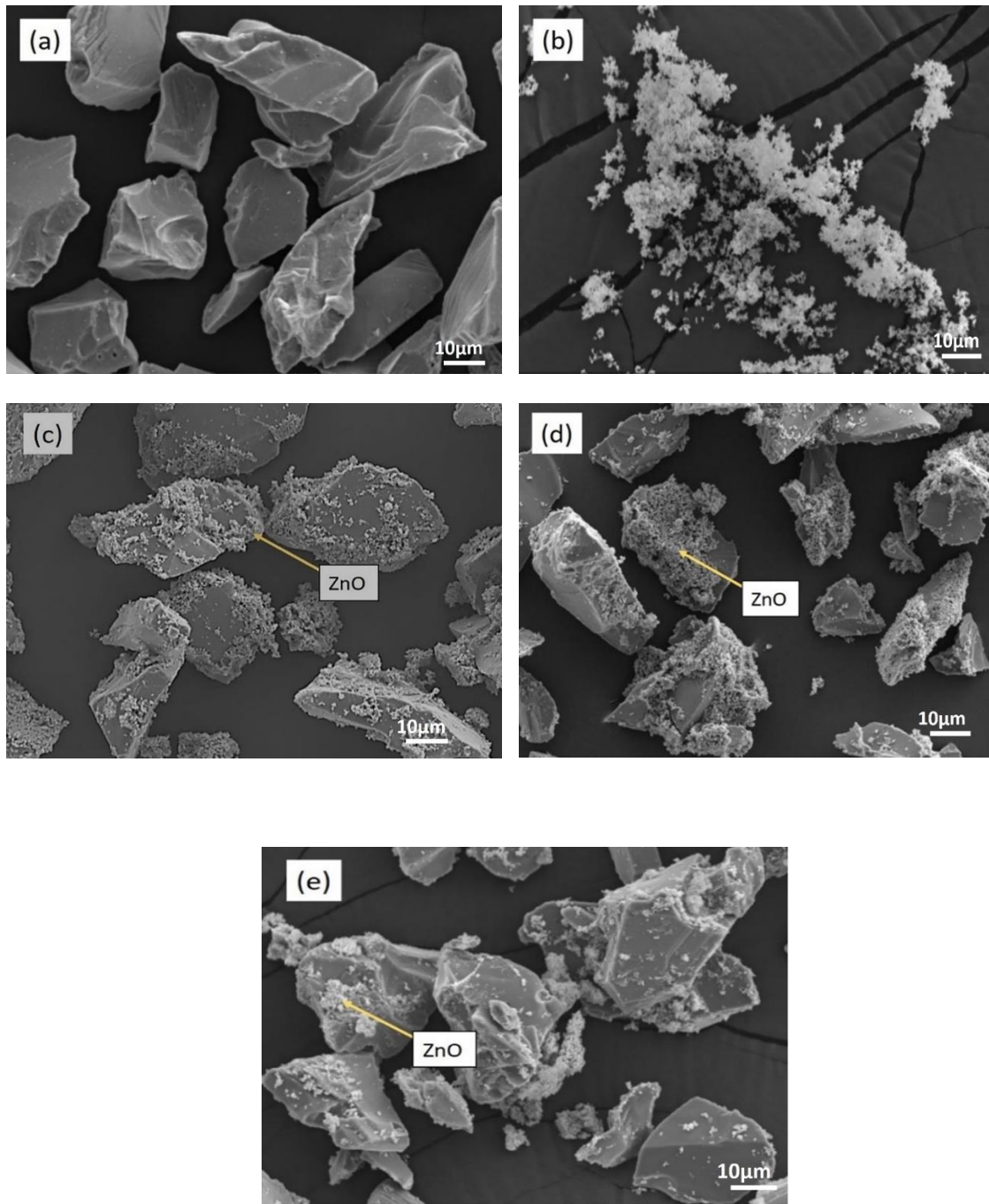
The surface morphology and particle characteristics of the TiO<sub>2</sub>/ZnO feedstock powders were investigated using field emission scanning electron microscopy (FESEM), as shown in Figure 4. The images reveal distinct morphological differences among the pure and mixed powders, which have implications for flowability, packing, and plasma spray performance.

Figure 4(a) shows the FESEM micrographs of pure TiO<sub>2</sub> powder, which exhibits relatively large, angular, and irregularly shaped particles with well-defined edges. The surfaces appear smooth with minimal porosity, indicating good packing potential and predictable flow behaviour. The sharp edges and faceted morphology are characteristic of Metco 102 TiO<sub>2</sub> powder, consistent with its high-density ceramic nature. Figure 4(b) presents the pure ZnO powder, which appears as smaller, irregular aggregates with rough surfaces. The particles are more fragmented and loosely packed compared to TiO<sub>2</sub>. This morphology may contribute to lower bulk density and reduced flowability, suggesting that ZnO addition could influence the powder's injection behaviour in plasma spraying.

The FESEM micrographs of the TiO<sub>2</sub>/ZnO composite powders (Figures 4(c), 4(d) and 4(e)) show progressive changes in morphology with increasing ZnO content. In the 70 wt.% TiO<sub>2</sub>/30 wt.% ZnO sample (Figure 4(c)), the particles exhibit partial agglomeration, with ZnO appearing as clusters adhering to the TiO<sub>2</sub> surfaces. The mixture retains the angular features of TiO<sub>2</sub> while introducing rougher textures, potentially increasing interparticle friction. The 80 wt.% TiO<sub>2</sub>/20 wt.% ZnO sample (Figure 4(d)) displays a more uniform distribution of ZnO across TiO<sub>2</sub> particles, with smaller ZnO aggregates filling interstitial spaces between larger TiO<sub>2</sub> particles. This morphology suggests improved packing density and potentially enhanced flowability. Finally, the 90 wt.% TiO<sub>2</sub>/10 wt.% ZnO sample (Figure 4(e)) exhibits minimal agglomeration, with ZnO uniformly coating TiO<sub>2</sub> particles without significantly altering their original angular shape, indicating good compatibility and homogeneity in the blended powder.

Overall, FESEM micrographs observations indicate that ZnO incorporation affects particle size distribution, surface texture, and agglomeration behavior, with higher ZnO content increasing surface roughness and potential interparticle interaction. Difference in TiO<sub>2</sub>/ZnO ratio effect the agglomeration level as reported from other research paper [13]. The morphology of the 80 wt.% TiO<sub>2</sub>/20 wt.% ZnO mixture appears most favorable for feedstock performance, balancing particle uniformity, flowability, and packing density. These results provide visual confirmation that controlled ZnO addition can modify TiO<sub>2</sub> powder morphology, which may influence melting behaviour and deposition efficiency during plasma spraying.

The FESEM micrographs of the TiO<sub>2</sub>/ZnO composite at high magnification (Figure 5) reveals that the ZnO particles predominantly exhibit irregular, aggregated morphologies with a rough surface texture. Individual particles appear submicron in size, with a tendency to form loosely packed clusters. This surface roughness and aggregation behaviour can influence powder flowability and packing density when used as a feedstock in plasma spraying, potentially affecting deposition efficiency and coating uniformity. EDX analysis is also used to further support the SEM finding on the TiO<sub>2</sub>/ZnO feedstock powder agglomeration (Figure 6). The EDX analysis shows that titanium and zinc element does present following the weight percentage ratio that is used. Oxygen element also exists due to both titanium and zinc oxide layer. The carbon traces in EDX analysis are because of the usage of carbon tape in sample preparation.



**Figure 4:** FESEM micrographs of (a) Pure TiO<sub>2</sub>, (b) Pure ZnO, (c) 70 wt.%TiO<sub>2</sub>/ 30 wt.%ZnO, (d) 80 wt.%TiO<sub>2</sub>/ 20 wt.% ZnO, and (e) 90 wt.%TiO<sub>2</sub>/10 wt.% ZnO feedstock powders

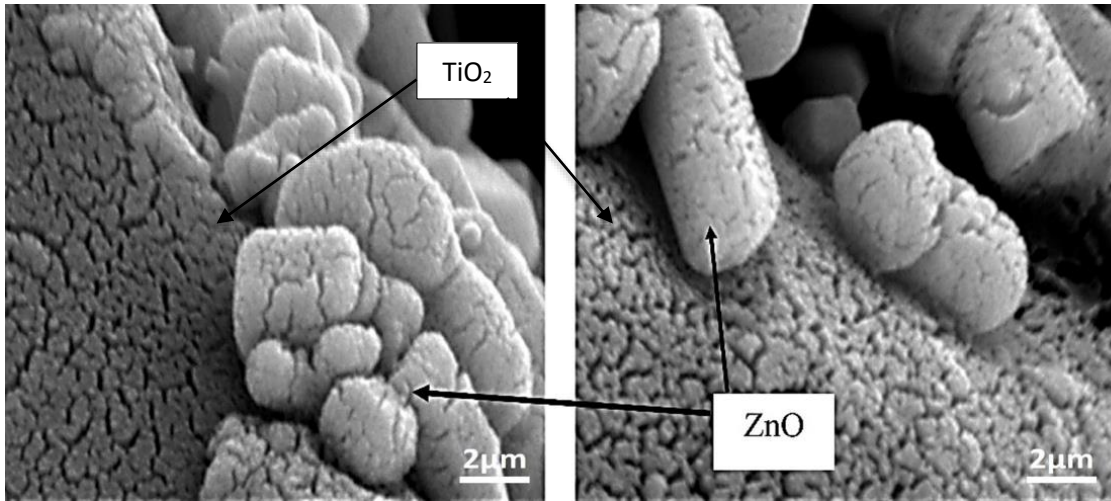


**Figure 5:** FESEM micrographs of ZnO powder exhibiting irregular, rough-surfaced particles and moderate agglomeration.

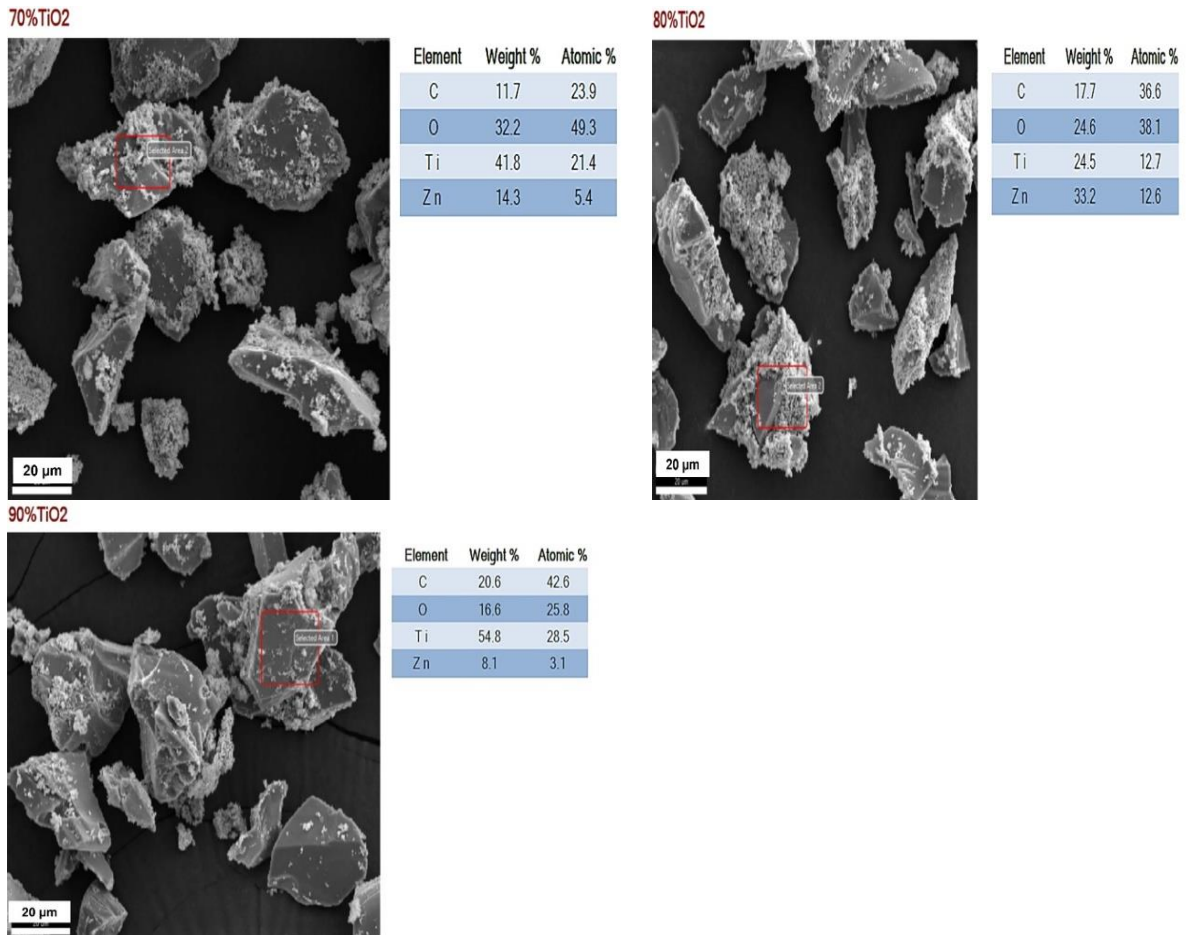


**Figure 6:** EDX analysis of TiO<sub>2</sub>/ZnO feedstock powder

### 3.2 Phase Analysis of TiO<sub>2</sub>/ZnO Feedstock Powders

The X-ray diffraction (XRD) patterns of pure TiO<sub>2</sub>, pure ZnO, and TiO<sub>2</sub>/ZnO composite powders with different compositions are presented in Figure 7. The diffraction peaks provide insight into the crystalline phases present and the influence of ZnO incorporation on the TiO<sub>2</sub> crystal structure. The diffraction pattern of pure TiO<sub>2</sub> powder exhibits strong and well-defined peaks corresponding to both anatase (A) and rutile (R) phases. The anatase phase (ICDD 00-021-1272) is identified by reflections at approximately  $2\theta = 37.65^\circ$ ,  $53.79^\circ$ , and  $68.9^\circ$ , while the rutile phase (ICDD 01-088-1173) is represented by reflections near  $2\theta = 36.3^\circ$ ,  $41.54^\circ$ , and  $54.8^\circ$ . These results indicate that the TiO<sub>2</sub> feedstock powder consists primarily of rutile TiO<sub>2</sub> with minor anatase content, which is typical for thermally processed TiO<sub>2</sub> powders used in coating applications. The pure ZnO powder, on the other hand, displays a distinct diffraction pattern characteristic of the wurtzite (Z) structure (ICDD 00-036-1451), with major peaks located at approximately  $31.7^\circ$ ,  $34.4^\circ$ , and  $36.2^\circ$ . The sharp and intense peaks confirm the high crystallinity of the ZnO feedstock powder.

In the TiO<sub>2</sub>/ZnO composite powders, the diffraction profiles exhibit prominent ZnO peaks with relatively weak or suppressed TiO<sub>2</sub> reflections. This is particularly evident as the ZnO content increases, where peaks corresponding to the wurtzite phase dominate the XRD pattern. Upon further analyzing, the sharp and high intensity of the ZnO peaks is mainly due to the atomic number of Zinc ( $Z=30$ ) that refract X-ray more effectively compared to Titanium ( $Z=22$ ) [14-15]. The absence of additional or shifted peaks indicates that no new crystalline phases were formed.

As the ZnO content decreases (e.g., 90 wt.% TiO<sub>2</sub>/10 wt.% ZnO), the intensity of ZnO peaks correspondingly reduces, while TiO<sub>2</sub> reflections become more discernible, indicating good compositional control and phase retention across all feedstock mixtures. The coexistence of distinct TiO<sub>2</sub> (anatase/rutile) and ZnO (wurtzite) peaks demonstrates effective physical blending and homogeneity of the composite powders. The dominance of ZnO peaks in the composite patterns is consistent with previous findings, where ZnO's higher diffractive intensity and uniform coating on TiO<sub>2</sub> surfaces tend to overshadow the TiO<sub>2</sub> signals in mixed systems. This observation supports that the feedstock produced is well agglomerated and homogeneously dispersed, ensuring stable structural integrity for subsequent plasma spray deposition.

XRD analysis confirmed that the ZnO powder crystallizes in the wurtzite phase, with sharp and well-defined peaks indicating high crystallinity. The wurtzite hexagonal lattice features strong tetrahedral ZnO bonding contributes to the observed particle stability and hardness, which are desirable for thermal spray applications [16]. The combination of submicron particle size, rough surface morphology, and wurtzite crystallinity suggests that the ZnO powder can provide enhanced nucleation sites when blended with TiO<sub>2</sub>, promoting better interparticle interactions and potentially improving coating density and adhesion [17]. These characteristics underscore the suitability of ZnO as a functional additive for optimizing multi-oxide plasma spray feedstocks.

In summary, the XRD analysis confirms the presence of both TiO<sub>2</sub> and ZnO crystalline phases in the composite feedstock powders, with ZnO exhibiting higher peak intensities due to its crystalline dominance and surface coverage on TiO<sub>2</sub> particles. The absence of new intermediate phases further indicates chemical stability and phase compatibility between TiO<sub>2</sub> and ZnO under the current preparation conditions [18].

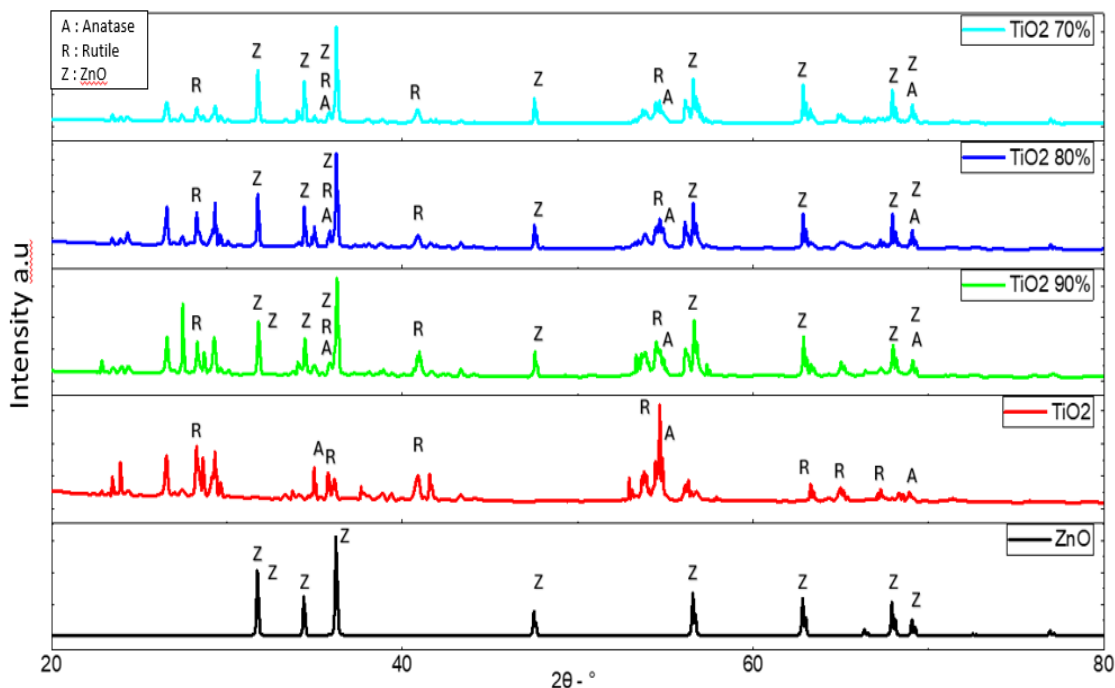


**Figure 7:** XRD patterns of pure TiO<sub>2</sub>, pure ZnO, and TiO<sub>2</sub>/ZnO composite feedstock powders with different ZnO contents

### 3.3 Particle Size Analysis

In order to investigate the particle size distribution of the TiO<sub>2</sub>/ZnO feedstock granules generated, a Particle Size Analyser (PSA, Malvern Mastersizer 2000) were used. The purified TiO<sub>2</sub> and ZnO powders had median particle diameters ( $d_{0.5}$ ) of 32.986  $\mu\text{m}$  and 13.289  $\mu\text{m}$ , respectively. The  $d_{0.5}$  values were 33.724  $\mu\text{m}$ , 32.047  $\mu\text{m}$ , and 32.800  $\mu\text{m}$  when TiO<sub>2</sub> and ZnO were combined in weight ratios of 90 wt.% TiO<sub>2</sub>/10 wt.% ZnO, 80 wt.% TiO<sub>2</sub>/20 wt.% ZnO and 70 wt.% TiO<sub>2</sub>/30 wt.% ZnO respectively, using a planetary ball mill (Retsch PM100). The consistent distribution of ZnO on the TiO<sub>2</sub> surface during mixing, as evidenced by the uniformity of particle size across all compositions shown in Figure 8, suggests that there was no substantial particle fragmentation or agglomeration. The SEM micrograph in Figure 8 also provides physical evidence of the structural stability of the feedstock; the sharp, angular facets of the TiO<sub>2</sub> core remain clearly defined, confirming that the mixing process did not result in particle fragmentation. Furthermore, the ZnO particles are observed to be uniformly 'decorated' across the core surface rather than forming isolated clusters, demonstrating a lack of significant agglomeration.

Powder flow and adhesion efficacy are substantially influenced by particle size in plasma spray applications. Excessively fine granules demonstrate poor flow characteristics as a result of the reduced apparent density and the increased cohesive forces associated with particles [19-20]. The particle sizes that were obtained are within the range that the manufacturer has designated as optimal for feedstock (~31.6  $\mu\text{m}$ ), which enables the consistent delivery of plasma jets and the seamless feeding of powder. Previous research has demonstrated that coatings with low porosity (2.13–3.89 %) and superior surface uniformity are typically produced by granules within this size range [21]. Consequently, the TiO<sub>2</sub>/ZnO feedstock powders generated in this investigation are anticipated to exhibit consistent coating performance and possess appropriate particle characteristics for efficient plasma spraying [22].

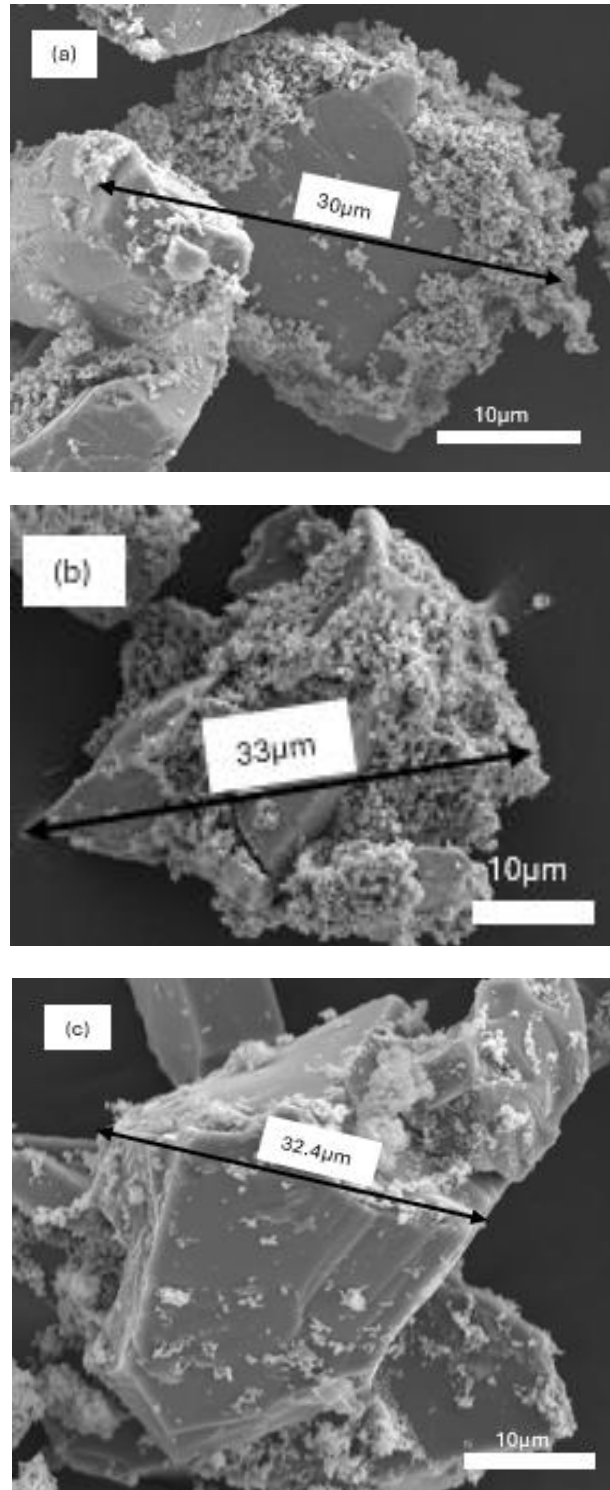


**Figure 8:** FESEM micrographs illustrating varied particle sizes of (a) 70 wt.%TiO<sub>2</sub>/ 30 wt.%ZnO, (b) 80 wt.%TiO<sub>2</sub>/ 20 wt.% ZnO, and (c) 90 wt.%TiO<sub>2</sub>/10 wt.% ZnO feedstock powders

### **3.4 Apparent Density Analysis of TiO<sub>2</sub>/ZnO Composite Feedstock Powders**

The apparent density of the TiO<sub>2</sub>/ZnO feedstock powders was measured to assess their suitability for plasma spray applications, as shown in Figure 9. Apparent density is a key indicator of powder packing efficiency, which directly affects coating quality, deposition efficiency, and microstructural integrity. Apparent density is the density of a material in its loose state. According to

ASTM B212, it represents the mass of powder per unit bulk volume, including the voids between particles. In this study, measurements were performed using approximately 50 g of powder gently filled into a 50 mL graduated cylinder, and the apparent density was calculated based on the recorded bulk volume. For verification, a complementary Archimedes-based test was conducted, where the displacement of water volume was used to determine powder volume and subsequently its density.

The results indicate that pure ZnO powder exhibits the highest apparent density among all samples. This finding suggests that ZnO particles possess a more compact packing structure with less interparticle voids. In contrast, pure TiO<sub>2</sub> powder shows significantly lower apparent density, attributed to its irregular particle morphology, which lead to looser packing. For the mixed TiO<sub>2</sub>/ZnO powders, the apparent density decreases progressively with increasing ZnO content. The 90 wt% TiO<sub>2</sub> /10 wt% ZnO sample records the highest density among the composites, followed by the 80 wt% TiO<sub>2</sub> /20 wt% ZnO and 70 wt% TiO<sub>2</sub> /30 wt% ZnO samples.

In this study, it was observed that increasing the ZnO content led to a reduction in the density of powder mixture, with the 90 wt.% TiO<sub>2</sub> /10 wt.% ZnO sample exhibiting the highest density among the samples. This behavior is attributed to packing disruption caused by the incorporation of smaller ZnO particles into the larger TiO<sub>2</sub> matrix, which hinders the particles from achieving a highly compact arrangement [23]. This trend implies that moderate ZnO addition (10 wt.%) minimizes the disruption, while excessive ZnO content may disrupt uniform packing due to particle size mismatch or agglomeration [24]. The lack of uniform packing makes the feedstock powder less dense. Since higher feedstock powder density is generally associated with lower coating porosity and improved mechanical performance, the 90 % TiO<sub>2</sub> feedstock powder is expected to yield coatings with higher hardness and superior wear resistance. These findings align with previous reports that denser feedstock powders contribute to more homogeneous and durable plasma-sprayed coatings.

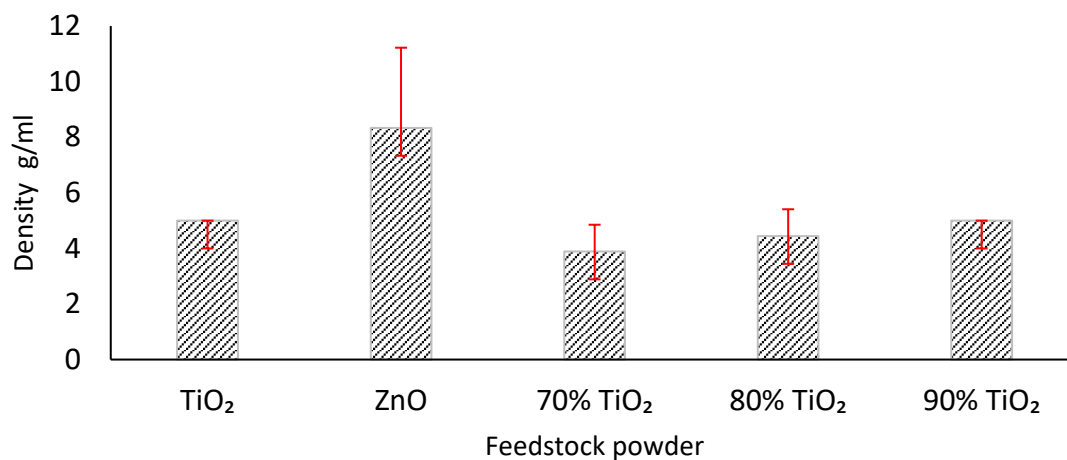


**Figure 9:** Apparent density results for TiO<sub>2</sub>/ZnO feedstock powders

#### 4. CONCLUSIONS

This study comprehensively evaluated the influence of ZnO addition on the physical and microstructural properties of TiO<sub>2</sub> based plasma spray feedstock powders. Through meticulous wet-mixing and agglomeration of the ingredients, TiO<sub>2</sub>/ZnO powder composites were produced with a consistent particle size distribution and morphology suitable for thermal spraying. XRD analysis indicated that anatase, rutile, and wurtzite phases can coexist simultaneously without the formation of a secondary phase as to synthesized TiO<sub>2</sub>-ZnO. This indicates that ZnO is uniformly distributed. SEM scans revealed that pure TiO<sub>2</sub> exhibited well-defined, angular particles, whereas ZnO displayed smaller,

irregular aggregates. Incorporating additional ZnO altered the morphology of the powder: at 10 wt.% ZnO, minimal agglomeration occurred, resulting in a uniform ZnO coating. At elevated ZnO concentrations ( $\geq 20$  wt.%), the surface exhibited increased roughness, and certain particles agglomerated, altering their interactions and packing behaviour. The apparent density measurements indicated that the incorporation of a moderate quantity of ZnO (10 wt.%) enhanced the bulk density and the packing efficiency of the powder. Nevertheless, excessive addition of ZnO reduced the density due to the formation of additional voids. The 90/10 composition exhibited the optimal amalgamation of phase stability, particle morphology, size distribution, and bulk density. These results provide critical insights into the customisation of multi-oxide ceramic powders to enhance coatings and improve deposition performance in advanced thermal spray applications.

## Acknowledgements

The authors would like to express their sincere gratitude to the Ministry of Higher Education Malaysia (MOHE) for the financial support under the Fundamental Research Grant Scheme (FRGS) [Grant No.: FRGS/1/2024/TK10/UTEM/02/4(KPT) and FRGS/1/2024/FTKIP/F00568(UTeM)], and to Universiti Teknikal Malaysia Melaka (UTeM) for providing the research facilities and technical assistance throughout this study.

## Author Contributions

All authors contributed toward data analysis, drafting and critically revising the paper and agree to be accountable for all aspects of the work.

## Disclosure of Conflict of Interest

The authors have no disclosures to declare.

## Compliance with Ethical Standards

The work is compliant with ethical standards.

## References

- [1] Michalak, M., Łatka, L., Sokołowski, P., Candidato, R. T. & Ambroziak, A. (2021). Effect of TiO<sub>2</sub> on the microstructure and phase composition of Al<sub>2</sub>O<sub>3</sub> and Al<sub>2</sub>O<sub>3</sub>-TiO<sub>2</sub> APS sprayed coatings. *Bulletin of the Polish Academy of Sciences: Technical Sciences*, 69(2), 1-9.
- [2] Yusuf, Y., Ghazali, M. J., Juoi, J. M., Rahim, T. A. & Mustafa, Z. (2022). Plasma-sprayed TiO<sub>2</sub> coatings: Hydrophobicity enhanced by ZnO additions. *International Journal of Applied Ceramic Technology*, 19(4), 2213-2221.
- [3] Omar, N. I., Yamada, M., Yasui, T. & Fukumoto, M. (2021). Bonding mechanism of cold-sprayed TiO<sub>2</sub> coatings on copper and aluminum substrates. *Coatings*, 11(11), 1349.
- [4] Grimm, M., Conze, S., Berger, L. M., Paczkowski, G., Lindner, T. & Lampke, T. (2020). Microstructure and sliding wear resistance of plasma sprayed Al<sub>2</sub>O<sub>3</sub>-Cr<sub>2</sub>O<sub>3</sub>-TiO<sub>2</sub> ternary coatings from blends of single oxides. *Coatings*, 10(1), 42.

- [5] Sani, M.A.M. & Yusuf, Y. (2025). Advances in TiO<sub>2</sub>-based composite coatings: Phase control, deposition methods and tribological performance. *Jurnal Tribologi*, 47, 183–200.
- [6] Shi, P., Sun, H., Yi, G., Wang, W., Wan, S., Yu, Y. & Wang, Q. (2023). Tribological behavior and mechanical properties of thermal sprayed TiO<sub>2</sub>-ZnO and TiO<sub>x</sub> ceramic coatings. *Ceramics International*, 49(11), 18662–18670.
- [7] Sridevi, K. P., Guru Prasad, L., Sangeetha, B., & Sivakumar, S. (2022). Structural and optical study of ZnO–TiO<sub>2</sub> nanocomposites. *Journal of Ovonic Research*, 18(3), 453–464.
- [8] Nassef, M. G. A., Nassef, B. G., Hassan, H. S., Nassef, G. A., Elkady, M. & Pape, F. (2024). Tribological and chemical–physical behavior of a novel palm grease blended with zinc oxide and reduced graphene oxide nano-additives. *Lubricants*, 12(6), 191.
- [9] Velumani, S., Tabares, J. A., Tsukanov, A., & Ossa, C. P. (2021). Engineered Zr/Zn/Ti oxide nanocomposite coatings for multifunctionality. *Applied Surface Science*, 563, 150353.
- [10] Gamez, J., Reyes-Osorio, L., Zapata, O., Cabriales, R., Lopez, L. & Delgado-Pamanes, M. (2024). Study of protective hard coatings of SiO<sub>2</sub>-TiO<sub>2</sub> on aluminum substrates. *AIMS Materials Science*, 11(2), 200–215.
- [11] Mahade, S., Venkat, A., Curry, N., Leitner, M. & Joshi, S. (2021). Erosion performance of atmospheric plasma sprayed thermal barrier coatings with diverse porosity levels. *Coatings*, 11(1), 86.
- [12] Kubaszek, T., Góral, M., & Pędrak, P. (2022). Influence of air plasma spraying process parameters on the thermal barrier coating deposited with micro- and nanopowders. *Materials Science–Poland*, 40(3), 80–92.
- [13] Krishnan, T., Nie, N. C., Abdullah, W. R. W., Awang, M. & Mansor, W. S. W. (2023). Titanium dioxide sol–gel/zinc oxide powder-coated clay beads in photocatalytic reactor. *Jurnal Teknologi*, 85(1), 71–79.
- [14] Nakayama, M., Akasaka, H., Sasaki, R. & Geso, M. (2024). Titanium dioxide-based nanoparticles to enhance radiation therapy for cancer: A literature review. *Journal of Nanotheranostics*, 5(2), 60–74.
- [15] Alvizuri-Tintaya, P. A., D’Abzac, P., Lo-Iacono-Ferreira, V. G., Torregrosa-López, J. I. & Lora-García, J. (2024). Zinc recovery from a water supply by reverse osmosis operated at low pressures: Looking for sustainability in water treatment advanced processes. *Membranes*, 14(6), 131.
- [16] Hossain, M. Z., Nayem, S. M. A., Alam, M. S., Islam, M. I., Seong, G. & Chowdhury, A. N. (2025). Hydrothermal ZnO nanomaterials: Tailored properties and infinite possibilities. *Nanomaterials*, 15(8), 609.
- [17] Anaya-Zavaleta, J. C., Ledezma-Perez, A. S., Gallardo-Vega, C., Rodriguez-Hernandez, J., Alvarado-Canche, C. N., Garcia-Casillas, P. E., De Leon, A. & Herrera-May, A. L. (2025). ZnO nanoparticles by hydrothermal method: Synthesis and characterization. *Technologies*, 13(1), 18.
- [18] Mohamed, W. M., Mohammed, Z. S. H., & Fadhil, M. A. (2024). Synthesis, characterization, structural, optical and photocatalyst properties of C60–ZnO–TiO<sub>2</sub> nano hybrid. *Journal of Nanostructures*, 14(1), 93–100.
- [19] Wang, H., Zhang, N., Wang, M. & Yang, F. (2024). Effect of particle size, lubricant, and heat temperature on the flowability of Ni-based powders for additive manufacturing. *Archives of Metallurgy and Materials*, 69(3), 1005–1014.

- [20] Rakhadilov, B., Berikkhan, K., Satbayeva, Z., Zhassulan, A., Shynarbek, A. & Ormanbekov, K. (2025). Optimization of cold gas dynamic spray coatings using agglomerated Al–Zn–TiO<sub>2</sub> powders on steel. *Metals*, 15(9), 1011.
- [21] Płatek, K., Łatka, L., Sokołowski, P., Kielczawa, T. & Sajbura, A. (2025). The effects of atmospheric plasma spray parameters on structure and mechanical properties of titanium dioxide coatings. *Advances in Science and Technology Research Journal*, 19(1), 381–389.
- [22] Kwon, H., Yoo, Y. W., Park, Y., Nam, U. H. & Byon, E. (2023). Effect of TiO<sub>2</sub> on mechanical and thermal properties of Al<sub>2</sub>O<sub>3</sub>-based coating via atmospheric plasma spraying. *Journal of Asian Ceramic Societies*, 11(2), 282–290.
- [23] Ashokan, A., Rajendran, S. & Dhairiyasamy, R. (2023). A comprehensive study on enhancing of the mechanical properties of steel fiber-reinforced concrete through nano-silica integration. *Scientific Reports*, 13(1), 20092.
- [24] Mohammed, M., Oleiwi, J. K., Jawad, A. J. M., Mohammed, A. M., Osman, A. F., Rahman, R., Adam, T., Betar, B. O., Gopinath, S. C. B., & Dahham, O. S. (2023). Effect of zinc oxide surface treatment concentration and nanofiller loading on the flexural properties of unsaturated polyester/kenaf nanocomposites. *Heliyon*, 9(9), e20051.